Illumination-Prior-Based High-Resolution DEM Reconstruction from Single-View Lunar Image Constrained with Initial DEM

Siyi Qiu [1], Zhen Ye [1, 2] *, Rong Huang [1, 2], Yusheng Xu [1, 2], Xiaohua Tong [1, 2]

[1] College of Surveying and Geoinformatics, Tongji University, Shanghai, China
[2] Shanghai Key Laboratory of Space Mapping and Remote Sensing for Planetary Exploration, Shanghai, China

Keywords: High-Resolution Digital Elevation Model, Lunar South Pole, Illumination Priors, Monocular Terrain Reconstruction, Initial DEM Constraint

Abstract

The lunar south pole is characterized by complex illumination conditions, extensive shadowed regions, and rugged topography, which make high-resolution terrain reconstruction from single-view imagery particularly challenging. To address this problem, this paper proposes an Illumination-Prior-Based DEM Reconstruction framework (IPDR) for single-view lunar terrain reconstruction under initial DEM constraints. The proposed method jointly exploits monocular image features, geometric prior information from the initial DEM, and illumination guidance derived from solar geometry. Experimental results on representative lunar south polar regions show that the proposed method achieves more stable and geometrically consistent reconstruction results than the compared methods. Large-area and local comparisons demonstrate improved terrain continuity and local morphological recovery, while ablation experiments verify the complementary roles of the initial DEM and the illumination prior. Additional experiments under different solar azimuth conditions and on ShadowCam imagery further show that the proposed framework maintains good robustness and adaptability. These results demonstrate the effectiveness of the proposed method for high-resolution lunar south polar terrain reconstruction from single-view imagery under initial DEM constraints.

1. INTRODUCTION

The lunar south pole has become a major target for future exploration because of its unique illumination environment, extensive permanently shadowed regions, and the potential presence of water ice. High-resolution digital elevation models (DEMs) are essential for geological interpretation, crater morphology analysis, landing-site selection, rover path planning, and resource assessment in this region (Zhou et al., 2024). However, accurate DEM reconstruction at the lunar south pole remains difficult because extremely low solar elevation angles, strong illumination contrasts, and rugged topography jointly degrade image texture and obscure reliable terrain cues, posing significant challenges for continuous and detailed terrain reconstruction (Okolie et al., 2022).

Existing terrain reconstruction approaches still show clear limitations under such conditions. Laser altimetry products such as LOLA provide reliable large-scale elevation constraints, but their spatial resolution is insufficient for recovering fine-scale topographic structures, especially in shadowed regions and along steep crater walls. Photogrammetric methods can generate accurate terrain models when high-quality stereo observations are available, yet such data are difficult to obtain in polar areas because of unfavorable imaging geometry and limited overlap (Jiménez-Jiménez et al., 2021). Shape-from-Shading (SfS) methods can recover local morphology from single-view imagery, but their performance is highly sensitive to shadows, albedo variations, and self-occluded slopes, which are common in the lunar south polar environment (Jia et al., 2025; Wu et al., 2018).

Recent learning-based monocular reconstruction methods have demonstrated the potential of estimating terrain geometry directly from single-view images (Yang et al., 2024a; Yang et al., 2024b). Nevertheless, their application to the lunar south pole remains challenging. In weakly illuminated regions, severe texture loss reduces the availability of reliable visual cues, leading to unstable elevation estimation and insufficient detail recovery. At the same time, the strong relief and frequent terrain transitions in polar craters make the mapping between image brightness and surface geometry more complex, which further limits model robustness and generalization (Jiao et al., 2020; Li et al., 2023). Although some dual-input frameworks incorporate auxiliary DEM information to alleviate scale ambiguity, they still struggle to maintain stable reconstruction quality in texture-degraded and strongly varying illumination conditions (Huang et al., 2025; Liu et al., 2022).

These challenges indicate that two issues must be addressed simultaneously for lunar south pole reconstruction. On the one hand, a reconstruction model should preserve the global terrain structure and absolute elevation trend rather than relying solely on image appearance. On the other hand, it should make better use of illumination-related cues to improve terrain recovery in shadowed and texture-degraded regions (Qian et al., 2025). Therefore, effectively integrating an initial DEM prior with illumination-aware image modeling is critical for achieving stable and detailed high-resolution DEM reconstruction from single-view lunar imagery (Gao et al., 2025). This is particularly important in shadowed areas, crater rims, and terrain-transition zones, where both geometric ambiguity and detail loss are severe.

To address these issues, this paper proposes an Illumination-Prior-Based DEM Reconstruction framework (IPDR) for high-resolution terrain reconstruction at the lunar south pole. The proposed method takes a single-view optical image and an initial DEM as inputs. The initial DEM provides coarse but reliable geometric constraints for the global terrain structure, while the illumination prior derived from solar geometry is used to guide

* Corresponding author

https://doi.org/10.5194/isprs-archives-XLIX-B2-2026-523-2026

feature learning in weak-texture and shadowed regions. By jointly exploiting monocular image features, initial terrain priors, and illumination information, the proposed framework improves the continuity, stability, and local detail recovery of reconstructed DEMs under complex polar illumination conditions.

The main contributions of this work are summarized as follows.
(1) An illumination-prior-based DEM reconstruction framework is proposed for single-view lunar terrain reconstruction under initial DEM constraints, aiming to improve reconstruction stability in the challenging environment of the lunar south pole.
(2) A joint reconstruction strategy is developed to combine monocular image features, coarse geometric priors from the initial DEM, and illumination-aware guidance, enabling better recovery in shadowed and terrain-transition regions.
(3) Comparative experiments, ablation analysis, and an additional ShadowCam case study demonstrate that the proposed method achieves more stable and geometrically consistent reconstruction results than existing approaches under complex illumination conditions.

2. METHOD

2.1 Overview

To address the difficulties of terrain reconstruction at the lunar south pole under extreme illumination conditions and rugged topography, we propose an Illumination-Prior-Based DEM Reconstruction framework (IPDR), as shown in Figure 1. The proposed framework aims to achieve stable and detailed high-resolution DEM reconstruction from single-view lunar imagery by jointly exploiting monocular image information, initial terrain priors, and illumination guidance.

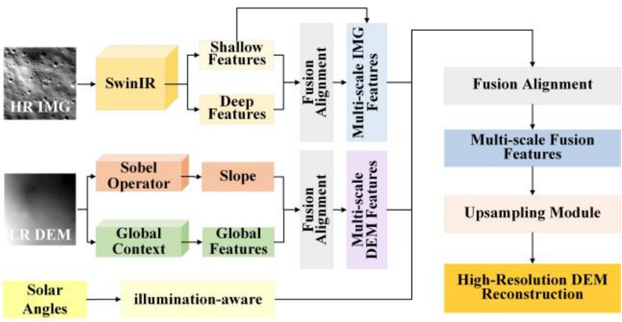

Figure 1. Overall architecture of the proposed IPDR framework.

The IPDR framework takes two inputs, namely a single-view optical image and an initial DEM. The optical image provides local texture, shading, and structural cues related to surface morphology, while the initial DEM offers coarse but reliable geometric information that constrains the large-scale terrain configuration. In addition, an illumination prior derived from solar geometry is introduced to provide auxiliary guidance in shadowed or texture-degraded regions, where image features alone are often insufficient for stable terrain reconstruction. The image features, DEM priors, and illumination guidance are subsequently fused to reconstruct the final high-resolution DEM.

Specifically, the framework consists of three main steps. First, the initial DEM is encoded to extract multi-level geometric priors for stabilizing the global elevation trend. Second, the monocular image is processed to extract terrain-related visual features, while the illumination prior is used to enhance feature learning under complex lighting conditions. Third, the geometric priors, image features, and illumination guidance are fused through a cross-modal alignment process and decoded into the reconstructed DEM, thereby improving geometric consistency and terrain recovery in shadowed and terrain-transition regions.

2.2 Illumination-Prior-Constrained Reconstruction

The core idea of the proposed method is to combine the complementary advantages of the initial DEM and the single-view image under illumination-aware guidance. On the one hand, the initial DEM provides a stable large-scale terrain skeleton and absolute elevation trend, which helps reduce the geometric ambiguity commonly encountered in monocular reconstruction. On the other hand, the optical image contains local morphological cues, such as brightness variations, texture transitions, and terrain boundaries, which are important for recovering fine-scale topographic structures. However, under lunar south polar illumination, such visual information is often incomplete or unreliable in shadowed and weak-texture areas. Therefore, illumination guidance is introduced to improve the utilization of image features in these challenging regions.

In the proposed framework, the initial DEM is first passed through a terrain encoder to extract coarse geometric priors. These priors mainly characterize the overall elevation distribution and large-scale terrain morphology, providing a stable structural reference for subsequent reconstruction. In parallel, the single-view image is fed into an image feature extraction branch to learn local terrain-related representations from available texture and shading patterns. To further enhance robustness, an illumination prior derived from solar geometry is incorporated during feature learning. Instead of using illumination information only as an external descriptor, the proposed method uses it as guidance for distinguishing reliable and unreliable visual cues under nonuniform lighting conditions, thereby improving feature discrimination in shadowed or texture-degraded regions.

After feature extraction, the geometric priors from the initial DEM, the visual features from the monocular image, and the illumination-aware guidance are integrated through a cross-modal alignment and fusion process. This process is designed to learn the coupled relationship among image intensity, terrain geometry, and illumination variation, so that the model can make better use of complementary information from different inputs. In this way, the initial DEM constrains the global terrain structure, the image branch provides local detail cues, and the illumination prior improves robustness under shadowed and weakly illuminated conditions. The fused representation is then decoded to generate the reconstructed DEM with improved geometric consistency and local terrain detail.

For clarity, the reconstruction process can be formulated in a compact form. Given the input optical image I, the initial DEM D_0, and the illumination prior P, the image feature is first guided by the illumination prior as follows.

$$F_i^g = \Psi(F_i, P), F_i = E_i(I) \tag{1}$$

where $E_i(\cdot)$ denotes the image encoder, F_i is the original image feature, and F_i^g is the illumination-guided image feature. Here, $\Psi(\cdot)$ represents the guidance operation that enhances feature representation in shadowed or texture-degraded regions under complex illumination conditions.

Meanwhile, the initial DEM is encoded to provide geometric prior information.

$$F_d = E_d(D_0) \tag{2}$$

This contribution has been peer-reviewed.
https://doi.org/10.5194/isprs-archives-XLIX-B2-2026-523-2026 | © Author(s) 2026. CC BY 4.0 License.

where $E_d(\cdot)$ denotes the DEM encoder and F_d represents the terrain prior feature extracted from the initial DEM.

The final reconstruction is then obtained by jointly integrating the DEM prior, the illumination-guided image feature, and the illumination information.

$$D_r = G\left(F_d, F_i^g, P\right) \quad (3)$$

where D_r denotes the reconstructed DEM and $G(\cdot)$ denotes the reconstruction function. In this formulation, the initial DEM constrains the global terrain structure, the image feature provides local morphological cues, and the illumination prior improves feature utilization under shadowed and weakly illuminated conditions.

2.3 Loss Function

For network optimization, a compact loss function is adopted to balance elevation reconstruction accuracy and terrain-structure consistency. The first term is a reconstruction loss that constrains the pixel-wise difference between the predicted DEM and the reference DEM, ensuring the overall numerical accuracy of elevation estimation. The second term is a gradient consistency loss that constrains local terrain variations, helping preserve slope changes and topographic transitions while reducing over-smoothing effects in complex terrain areas. The overall loss function can be written as follows.

$$L = \lambda_1 L_{rec} + \lambda_2 L_g \quad (4)$$

where L_{rec} denotes the elevation reconstruction loss, L_g denotes the gradient consistency term, and λ_1 and λ_2 are balancing coefficients.

3. EXPERIMENTS AND RESULTS

3.1 Data and Experimental Settings

To evaluate the effectiveness of the proposed IPDR method, experiments were conducted on representative regions in the lunar south pole. The training dataset contains samples with diverse terrain types and illumination conditions, enabling the model to learn reconstruction patterns under different topographic and radiometric situations. The training data were extracted from the lunar south polar region between 87°S and 90°S and cropped into fixed-size patches, resulting in approximately 1,500 paired samples. Each sample includes a low-resolution LOLA DEM patch, a corresponding single-view optical image patch, and a reference high-resolution DEM used as supervision during training. The test data were selected from regions different from the training area, including representative sites around (37°E, -85°S) and (125°E, -88°S), in order to evaluate the performance of the proposed method on unseen terrain.

Before training and inference, all data were preprocessed through co-registration, normalization, and resampling to ensure spatial consistency between the optical image and the initial DEM (Chen et al., 2023). The initial DEM was generated from LOLA data and used as the geometric prior for reconstruction, while the reference DEM served as the supervision target for model training and quantitative evaluation (Barker et al., 2023). In addition, independent LOLA laser altimetry points were used for external validation of the reconstructed results (Hemmi et al., 2025). This evaluation setup makes it possible to assess not only the agreement between the predicted DEM and the reference terrain product, but also the geometric reliability of the reconstruction with respect to independent measurements.

Comparative experiments were conducted against representative existing methods, including MADNet, ELunarDTMNet, and the SfS method (Chen et al., 2024; Liu et al., 2022; Tao et al., 2023; Ye et al., 2025). For the comparison of different reconstruction methods, four metrics were adopted, including $RMSE_e$, $RMSE_s$, $RMSE_a$ (in degrees), and $RMSE_p$. Specifically, $RMSE_e$, $RMSE_s$, and $RMSE_a$ were computed with respect to the digital elevation model generated by SfS, and were used to evaluate the consistency of different reconstruction methods in terms of elevation accuracy, local terrain variation, and geomorphological direction preservation. By contrast, $RMSE_p$ was calculated against independent LOLA laser altimetry points and used as an external indicator of geometric reliability.

3.2 Reconstruction Results

A representative reconstruction result over a 5 km × 5 km south polar region is presented in Figure 2. The NAC image shows that the study area contains multiple small craters and subtle terrain undulations, while the corresponding LOLA DEM mainly preserves the large-scale elevation gradient of the region. In the LOLA hill-shaded view, the terrain appears relatively coarse, and many local geomorphological features are difficult to distinguish clearly. By comparison, the DEM reconstructed by the proposed IPDR framework preserves the overall topographic trend of the original terrain while recovering substantially richer local morphology. Small crater depressions, crater rims, and local slope transitions can be identified more clearly in the reconstructed DEM than in the initial LOLA DEM. This difference is especially evident in the zoomed-in hill-shaded comparison, where the LOLA result exhibits obvious block-like smoothing, whereas the IPDR result shows more recognizable crater morphology and finer local relief.

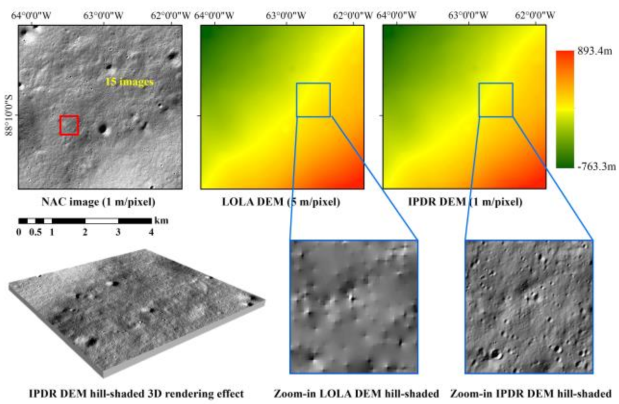

Figure 2. Large-Area Reconstruction Result over a 5 km × 5 km South Polar Region.

To further evaluate local reconstruction quality, the red-box region in Figure 2 was selected for detailed comparison, and the corresponding results of different methods are shown in Figure 3. In this region, the LOLA DEM provides only a very smooth surface and fails to represent many small-scale topographic structures visible in the image. MADNet and ELunarDTMNet recover part of the terrain variation, but their DEM and hill-shaded results still show incomplete local structure expression. In particular, in the red-box regions and the orange-circled areas, these methods tend to produce blurred crater boundaries, locally distorted terrain shapes, or insufficient expression of subtle depressions and rims. The proposed IPDR result preserves clearer crater edges, more coherent local depressions, and more natural slope transitions. Compared with the other learning-based methods, its hill-shaded representation is also more structurally stable in shadow-affected and texture-weak regions. Compared with SfS, the IPDR reconstruction maintains similarly recognizable small-scale terrain features while showing a more continuous and stable terrain surface in the selected area.

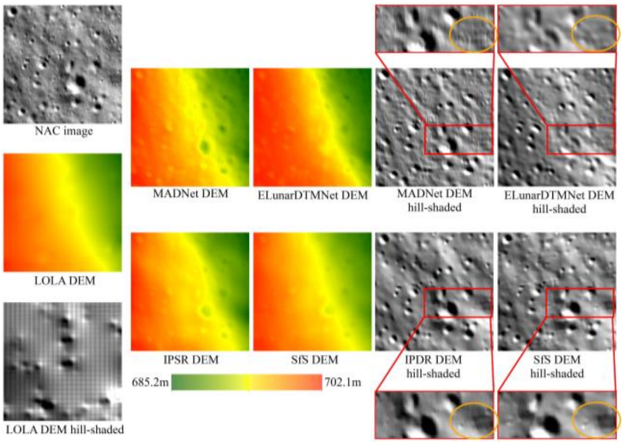

Figure 3. Visual Comparison of Different Reconstruction Methods in the Selected Local Region.

The corresponding quantitative comparison is reported in Table 1. The numerical evaluation is consistent with the visual observations from the local comparison. The proposed method achieves better performance in elevation-related and terrain-gradient-related metrics, and also shows more favorable validation results against independent LOLA laser altimetry points. This agreement between the visual comparison and the point-based validation supports that the improvement of the proposed method is not limited to appearance in hill-shaded rendering, but is also reflected in geometric accuracy. The regional reconstruction, local comparison, and quantitative evaluation consistently show that the proposed method preserves the main terrain pattern while improving local structural continuity and geometric accuracy.

Methods	$RMSE_e$	$RMSE_s$	$RMSE_a$	$RMSE_p$
MADNet	3.0846	4.4289	54.7321	1.9843
ELunarDTMNet	0.8725	3.2418	46.9137	1.1436
IPDR	0.5842	2.3174	37.9685	0.2478
SfS	Reference	Reference	Reference	0.2961

Table 1. Quantitative Evaluation of Different Reconstruction Methods in the Selected Local Region.

3.3 Ablation Study

To further examine the effectiveness of the key components in the proposed framework, an ablation study was conducted on the test regions. Considering the compact scope of this conference paper, three model settings were designed for comparison, including a baseline model using only the single-view image, a model combining the single-view image with the initial DEM, and the full IPDR model that jointly integrates the single-view image, the initial DEM, and the illumination prior. This experimental setting makes it possible to analyze, in a progressive manner, how the reconstruction performance changes when geometric prior information and illumination-aware guidance are introduced step by step. In this ablation study, the quantitative evaluation focuses on point-based geometric reliability. Therefore, three point-based metrics, namely $RMSE_p$, $Bias_p$, and MAE_p, are reported in Table 2, while the corresponding visual comparison results are presented in Figure 4. Among these metrics, $RMSE_p$ reflects the overall magnitude of point-wise elevation deviation, $Bias_p$ describes the systematic overestimation or underestimation of reconstructed elevations, and MAE_p measures the average absolute discrepancy between the reconstructed results and the LOLA laser altimetry observations.

	$RMSE_p$	$Bias_p$	MAE_p
Baseline (Image Only)	1.9738	1.6889	1.8321
Image + Initial DEM	1.1426	0.9364	1.0187
Full IPDR (Image + Initial DEM + Illumination Prior)	0.2369	0.0698	0.2014
SfS	0.2783	0.2217	0.2386

Table 2. Quantitative Ablation Results of Different Model Settings.

The quantitative ablation results show a clear improvement trend from the baseline model to the full IPDR model. When only the single-view image is used, the reconstruction result is more easily affected by weak texture, shadow interference, and illumination ambiguity, which leads to unstable terrain recovery and relatively large geometric deviation. After the initial DEM is introduced, the reconstruction becomes more stable at the large scale, and the overall terrain structure is better preserved. This indicates that the initial DEM provides an effective geometric constraint for monocular terrain reconstruction, especially in regions where image appearance alone is insufficient to determine reliable elevation variation. When the illumination prior is further incorporated in the full IPDR model, the reconstruction quality is improved again, particularly in regions with complex illumination, weak image texture, and terrain transition. This demonstrates that the illumination prior can further enhance the model's ability to utilize image cues under difficult lighting conditions.

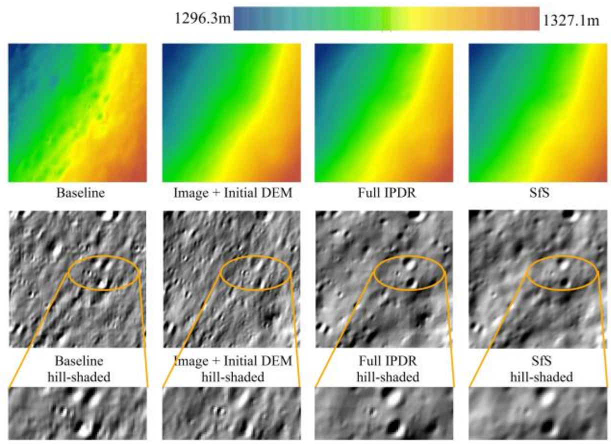

Figure 4. Visual Comparison of Different Ablation Settings.

The visual comparison in Figure 4 provides more intuitive evidence for the above observations. The baseline model tends to produce locally unstable terrain structures and incomplete recovery in weakly illuminated areas. After incorporating the initial DEM, the reconstructed terrain becomes more coherent, and the large-scale geomorphological pattern is better maintained. On this basis, the full IPDR model further improves the continuity of shadowed regions, the expression of crater boundaries, and the structural integrity of terrain-transition areas.

Compared with the other two settings, the full model shows fewer local artifacts and better preservation of terrain morphology, indicating that the illumination prior does not simply add local details, but helps stabilize the relationship between image appearance and terrain geometry in visually ambiguous regions.

The ablation results suggest that the initial DEM and the illumination prior play different but complementary roles in the proposed framework. The initial DEM mainly constrains the large-scale terrain configuration and suppresses global structural instability, whereas the illumination prior mainly improves feature utilization and local reconstruction reliability under complex lighting conditions. Their joint use enables the full IPDR model to achieve a more balanced reconstruction performance, preserving both the global terrain structure and the local morphological continuity of the lunar south polar surface.

3.4 Robustness under Different Solar Azimuth Conditions

To further evaluate the robustness of the proposed method under different illumination conditions, additional experiments were conducted under different solar azimuth angles. Since illumination variation strongly affects image appearance and the availability of terrain-related visual cues in the lunar south pole, this experiment is important for examining whether the proposed framework can maintain stable reconstruction quality when the lighting condition changes. Representative results under two solar azimuth settings are presented in Figures 5 and 6, corresponding to 60° and 300°, respectively.

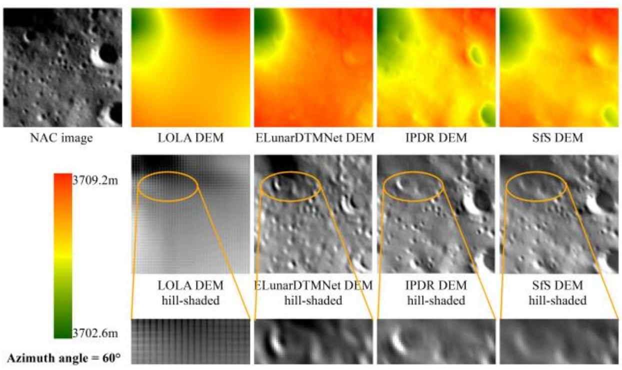

Figure 5. Reconstruction Results of Different Methods at a Solar Azimuth of 60°.

The results show that the proposed IPDR framework maintains relatively stable reconstruction performance under different illumination conditions. Under both solar azimuth settings, the reconstructed DEMs preserve the main terrain structure and remain more continuous than those produced by the compared methods. In particular, in weakly illuminated regions, crater boundaries, and terrain-transition areas, the proposed method is less affected by illumination-induced texture degradation and exhibits fewer local inconsistencies. This indicates that the proposed framework can make more effective use of terrain-related image cues when the lighting environment changes.

A comparison between Figures 5 and 6 further suggests that the proposed method is not overly sensitive to azimuth changes. Although the image appearance differs noticeably under the two illumination conditions, the reconstructed terrain produced by IPDR remains structurally consistent, and the main geomorphological features are preserved in both illuminated and shadowed areas. This behavior is particularly important for lunar south polar reconstruction, where the same terrain may be observed under substantially different solar geometries and where illumination variation can easily introduce ambiguity into image-based terrain interpretation. From the visual results, it can also be observed that the advantage of the proposed method is not limited to one specific local feature. Under both illumination settings, IPDR shows better continuity in shadowed regions, clearer expression of crater rims and slopes, and fewer local artifacts in areas with abrupt terrain transition. By contrast, the compared methods are more likely to suffer from structural instability or local distortion when terrain texture becomes weak or when the shadow distribution changes significantly. This difference suggests that the proposed strategy is able to maintain a more stable relationship between image features and terrain geometry under changing illumination conditions.

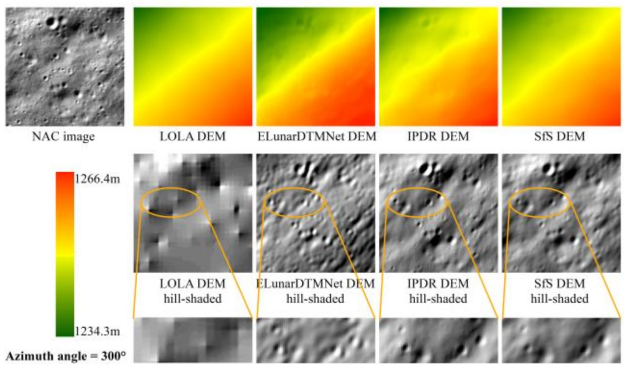

Figure 6. Reconstruction Results of Different Methods at a Solar Azimuth of 300°.

The above comparisons show that the proposed illumination-prior-based reconstruction strategy improves reconstruction stability under varying illumination conditions. The initial DEM provides stable large-scale geometric support, while the illumination prior helps the model better interpret terrain-related image information when the visual appearance changes with solar azimuth. Their joint use enables the proposed framework to maintain more stable reconstruction quality across different illumination settings.

3.5 Reconstruction Results on ShadowCam Imagery

To further examine the adaptability of the proposed framework to another image source, additional experiments were conducted using ShadowCam imagery. ShadowCam is a lunar orbital imaging sensor designed for weakly illuminated regions, and it is capable of capturing surface information in areas where conventional optical images are often less informative (Robinson et al., 2023). Compared with the NAC-based experiments in the previous sections, this part focuses on whether the proposed IPDR method can still produce reasonable terrain reconstruction results when the input image is replaced by ShadowCam imagery. The corresponding results are shown in Figure 7.

From the visual comparison, the proposed method remains capable of reconstructing the main terrain structure under the ShadowCam imaging condition. Although the image appearance differs from NAC imagery and the local contrast distribution is also different, the reconstructed DEM still preserves the overall geomorphological pattern of the selected region. Major topographic elements, such as crater depressions, crater boundaries, and local slope transitions, can still be recognized in the reconstructed result. In addition, the terrain surface generated by IPDR remains relatively continuous, without obvious large-area structural breakage.

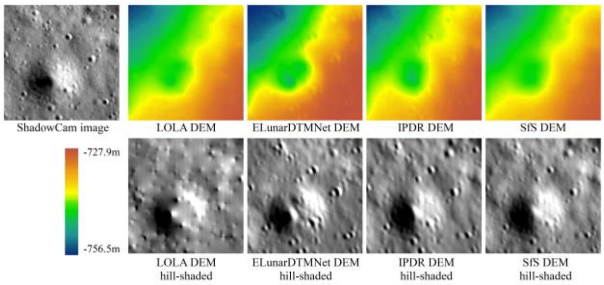

Figure 7. Visual Comparison of Reconstruction Results on ShadowCam Imagery.

A more detailed comparison further shows that the proposed method is able to retain meaningful local morphology in ShadowCam-based reconstruction. In regions with weak illumination or subtle terrain relief, the reconstructed result still exhibits identifiable local depressions and boundary structures, whereas coarse initial terrain alone would not be sufficient to describe these details. This indicates that the combination of initial DEM constraint and illumination prior can still support effective terrain recovery when the input image is replaced by ShadowCam imagery. The ShadowCam experiment therefore provides a supplementary validation of the proposed framework under a different imaging condition. Together with the NAC-based experiments, it further confirms that the proposed IPDR framework can maintain stable terrain reconstruction capability when applied to different lunar south polar image sources.

4. CONCLUSION

This paper proposes an Illumination-Prior-Based DEM Reconstruction framework (IPDR) for high-resolution terrain reconstruction in the lunar south pole from single-view optical imagery under initial DEM constraints. By jointly incorporating monocular image information, geometric support from the initial DEM, and illumination guidance derived from solar geometry, the proposed method improves terrain recovery in shadowed, weak-texture, and structurally ambiguous regions. Experimental results show that the proposed framework achieves better reconstruction performance than the compared methods in both visual and quantitative evaluations. Large-area and local reconstruction results confirm its ability to preserve the main terrain pattern while improving local morphological continuity and detail recovery. Ablation experiments verify the complementary roles of the initial DEM and the illumination prior, and additional experiments under different solar azimuth conditions and on ShadowCam imagery further demonstrate stable reconstruction capability under varying illumination and different image sources. These results support the effectiveness of the proposed framework for stable and detailed lunar south polar terrain reconstruction from single-view imagery under initial DEM constraints.

ACKNOWLEDGMENT

This work was supported by the National Natural Science Foundation of China under Grant Nos. 42571517 and 42221002.

REFERENCES

Barker, M.K., Mazarico, E., Neumann, G.A., et al., 2023. A new view of the lunar south pole from the Lunar Orbiter Laser Altimeter (LOLA). *Planet. Sci. J.*, 4(9), 183.

Chen, C., Ye, Z., Xu, Y., et al., 2023. Large-scale block bundle adjustment of LROC NAC images for lunar south pole mapping based on topographic constraint. *IEEE J. Sel. Top. Appl. Earth Obs. Remote Sens.*, 17, 2731-2746.

Chen, H., Gläser, P., Hu, X., et al., 2024. ELunarDTMNet: Efficient reconstruction of high-resolution lunar DTM from single-view orbiter images. *IEEE Trans. Geosci. Remote Sens.*, 62, 1-20.

Gao, B., Yue, L., Qiu, Z., et al., 2025. Exploring the integration of auxiliary modal information from remote sensing images for DEM super-resolution. *Int. J. Geogr. Inf. Sci.*, 39(12), 2886-2912.

Hemmi, R., Inoue, H., Kikuchi, H., et al., 2025. LROC NAC-derived meter-scale topography of the Moon's south polar landing sites: Digital terrain models and their quality assessments. *Planet. Sci. J.*, 6(11), 264.

Huang, R., Ding, W., Xu, Y., et al., 2025. Fusion of multiple photogrammetric DEMs for large-scale lunar topographic mapping. *Adv. Space Res.*, 75(6), 5227-5242.

Jia, R., Wu, B., Mahanti, P., 2025. Shape-from-shading with secondary illumination for 3D reconstruction of permanently shadowed regions at the lunar south pole. *Acta Astronaut.*, 238, 889-903.

Jiao, D., Wang, D., Lv, H., et al., 2020. Super-resolution reconstruction of a digital elevation model based on a deep residual network. *Open Geosci.*, 12(1), 1369-1382.

Jiménez-Jiménez, S. I., Ojeda-Bustamante, W., Marcial-Pablo, M. D. J., et al., 2021. Digital terrain models generated with low-cost UAV photogrammetry: Methodology and accuracy. *ISPRS Int. J. Geo-Inf.*, 10(5), 285.

Li, Z., Zhu, X., Yao, S., et al., 2023. A large-scale digital elevation model super-resolution Transformer. *Int. J. Appl. Earth Obs. Geoinf.*, 124, 103496.

Liu, Y., Wang, Y., Di, K., et al., 2022. A generative adversarial network for pixel-scale lunar DEM generation from high-resolution monocular imagery and low-resolution DEM. *Remote Sens.*, 14(21), 5420.

Okolie, C.J., Smit, J.L., 2022. A systematic review and meta-analysis of digital elevation model (DEM) fusion: Pre-processing, methods and applications. ISPRS J. *Photogramm. Remote Sens.*, 188, 1–29.

Qian, J., Ye, Z., Qiu, S., et al., 2025. Secondary scattering shape from shading for precise terrain reconstruction of the lunar permanently shadowed regions. *Icarus*, 431, 116494.

Robinson, M.S., Brylow, S.M., Caplinger, M.A., et al., 2023. ShadowCam instrument and investigation overview. *J. Astron. Space Sci.*, 40(4), 149-171.

Tao, Y., Muller, J.P., Conway, S.J., et al., 2023. Large area high-resolution 3D mapping of the von Kármán crater: Landing site for the Chang'E-4 lander and Yutu-2 rover. *Remote Sens.*, 15(10), 2643.

Wu, B., Liu, W.C., Grumpe, A., et al., 2018. Construction of pixel-level resolution DEMs from monocular images by shape and albedo from shading constrained with low-resolution DEM. *ISPRS J. Photogramm. Remote Sens.*, 140, 3-19.

Yang, L., Kang, B., Huang, Z., et al., 2024a. Depth anything: Unleashing the power of large-scale unlabeled data. *In: Proc. IEEE/CVF Conf. Comput. Vis. Pattern Recogn. (CVPR)*, 10371-10381.

Yang, L., Kang, B., Huang, Z., et al., 2024b. Depth anything v2. *Adv. Neural Inf. Process. Syst.*, 37, 21875-21911.

Ye, Z., Qian, J., Xu, Y., et al., 2025. Adaptive weighted multi-image shape from shading for precise topographic reconstruction at the lunar south pole. *Astron. J.*, 170(1), 31.

Zhou, M., Ye, Z., Huang, R., et al., 2024. High-resolution morphology of lunar lava tube pits using photogrammetric modeling of multiple stereo images. *Earth Space Sci.*, 11(11), e2024EA003532.